Korean J. Chem. Eng., 34(5), 1495-1499 (2017)
DOI: 10.1007/s11814-017-0041-1

pISSN: 0256-1115
eISSN: 1975-7220

Fabrication of NOA microfluidic devices based on sequential replica molding

Jae Hwan Sim, Hyun June Moon, Yoon Ho Roh, Hyun Wook Jung, and Ki Wan Bong†

Department of Chemical and Biological Engineering, Korea University, 145 Anam-ro, Seongbuk-gu, Seoul 02841, Korea

(*Received 13 November 2016 • accepted 14 February 2017*)

Abstract−Polydimethylsiloxane (PDMS) microfluidic devices, though they are commonly utilized in microfluidic applications, have several limitations, such as short-term modified surface condition, swelling in the presence of organic solvents, and deformation under high pressure or when built with low aspect ratios. To resolve the restrictions, Norland Optical Adhesive (NOA) has been introduced as an excellent alternative for PDMS. Here, we present a practical protocol for the fabrication of NOA microfluidic devices via a step-wise molding process. Through the indirect molding of NOA on wafers, the damage to the wafers can be significantly reduced. Furthermore, because we use positive-patterned wafers, which are commonly used to fabricate PDMS devices, no additional fabrication of the wafer is required. This simple strategy thus avoids damage to the wafers and simultaneously allows for the mass production of NOA devices without deformation. We also test the performance of NOA devices in oil-in-water droplet production and in a microfluidic process using organic solvents.

Keywords: NOA, UV Curable Resin, Microfluidics, Device Fabrication, Replica Molding

INTRODUCTION

The use of polydimethylsiloxane (PDMS) has been widespread in the fabrication of microfluidic devices [1]. By virtue of properties such as good optical transparency [2] and inherent elasticity [3], PDMS microfluidic devices allow for easy observation, minimal fluorescent decay, and facile binding to other mechanical components [4]. PDMS devices have also been adopted in bio-applications such as cell culturing, cell sorting, and biomimicry due to their high gas permeability and the biocompatibility of PDMS elastomers [5]. Practically, compared to other device fabrication methods, PDMS devices are easily produced via replica molding, which does not require sophisticated techniques or costly equipment [6]. Thanks to these advantages, PDMS devices have been widely used in various fields, including rheology [7-9], biochemistry [10-12], tissue engineering [13-15], medical engineering [16-19], and optics [20,21].

However, PDMS devices have several limitations. First, PDMS devices swell instantly when they come into contact with most organic solvents [22]. In addition, it is a challenging task that PDMS surface is modified to hydrophilic condition permanently [23,24]. Finally, due to the inherent low elastic modulus of PDMS, significant deformation can occur in certain situations. For example, PDMS devices bulge or even break under high pressure [25,26]. PDMS patterns with low aspect ratios also experience deformation in the form of sagging [27]. For these reasons, researchers have recently fabricated microfluidic devices using various materials such as thiolene-based resins [28,29], polycarbonate [30,31], Teflon [32], polyethylene glycol [33], polyimide [34,35], and polyurethane acrylate (PUA) [36,37] to overcome the limitations of PDMS devices.

Of the materials mentioned above, Norland Optical Adhesive (NOA), a thiolene-based resin, has been considered a promising material for a number of reasons. First, devices fabricated with NOA can tolerate most organic solvents due to its strong solvent resistance [38]. Secondly, long-lasting hydrophilic surface of NOA is relatively simple to be accomplished via conventional oxygen plasma treatment [39]. Finally, it is a rigid material with a Young's modulus of 325 MPa (~160 times higher than that of PDMS), which prevents deformation under high pressure and for devices with low aspect ratios. Moreover, the bonding strength of NOA (~560 kPa) is still two times stronger than that of PDMS [40]. Several methods for the fabrication of NOA devices have been introduced in previous studies. One of them is the direct molding of NOA using a patterned silicon wafer. In this method, NOA resin is poured onto a positive-patterned silicon wafer, cured, and separated to acquire patterned NOA blocks [41]. Unfortunately, due to the strong adhesion between NOA and the wafer, the wafer is often damaged by the stress exerted when the NOA replica is peeled away. To resolve this, Bartolo et al. [42] proposed the indirect patterning of NOA from the wafer. This methodology uses a positive-patterned PDMS mold to produce a negative-patterned NOA replica. However, given that positive-patterned wafers are predominantly used to fabricate PDMS devices, negative-patterned wafers have to be prepared in the method, which requires additional cost. Moreover, the negative-patterned wafer is vulnerable to wearing because most of its surface is comprised of a photoresist.

In this paper, we introduce a practical protocol for the fabrication of NOA microfluidic devices via sequential replica molding. We characterize the degree of deformation during the step-wise molding process. We also propose a simple strategy for the mass production of NOA microfluidic devices using a single negative-patterned PDMS replica. Furthermore, we demonstrate that NOA

†To whom correspondence should be addressed.
E-mail: bong98@korea.ac.kr

‡This article is dedicated to Prof. Ki-Pung Yoo on the occasion of his retirement from Sogang University.

Copyright by The Korean Institute of Chemical Engineers.

microfluidic devices fabricated via sequential molding have characteristics which enable them to be applied to areas where PDMS devices do not function well, such as oil-in-water droplet production and microfluidic operations using organic solvents.

MATERIALS AND METHODS

1. Materials

SU-8 photoresists for patterning on silicon wafers were purchased from MicroChem Corp., USA. A positive-patterned silicon wafer was fabricated via photolithography using SU-8. PDMS was purchased from Corning, USA. Norland Optical Adhesive (NOA) is the product of Norland Products. Tridecafluoro-1,1,2,2-tetrahydrooctyl trichlorosilane (silane) was supplied by Gelest, Inc., Morrisville PA. All of the chemicals were used as received without additional treatment.

2. Fabrication of NOA Microfluidic Devices via Sequential Replica Molding

2-1. Fabrication of the Negative-patterned PDMS Replica

A negative-patterned PDMS mold is fabricated via replica molding. To maximize the modulus of the PDMS mold, the PDMS is thoroughly mixed with a curing agent at a volumetric ratio of 9 : 1, instead of the typical 10 : 1, then the solution is poured over the silicon wafer [43]. After the complete removal of the air bubbles in the PDMS using a vacuum pump, thermal curing is conducted in an oven at 70 °C for 3 hours. Finally, the PDMS replica is separated from the wafer.

2-2. Fabrication of the Positive-patterned PDMS Replica

We mark the boundary of the negative-patterned PDMS template fabricated in the previous step. This template is attached to the substrate while the pattern is facing upward. The surface properties of the PDMS template are modified by the vapor deposition of silane. The deposition of silane changes the surface of the PDMS from hydrophobic to hydrophilic. The deposition of silane on PDMS treated by atmospheric plasma is performed in a desiccator with 0.25 bars for 90 min [44]. After removal from the vacuum, the PDMS and curing agent mixture (9 : 1) is poured on the silane-treated PDMS template. After curing in an oven, a positive-patterned PDMS mold is obtained in a similar fashion to the fabrication of the negative-patterned PDMS replica.

2-3. Fabrication of the NOA Microfluidic Device

The bottom layer of the NOA device is fabricated by gently sandwiching NOA resin between the positive-patterned PDMS replica and the slide glass. After the removal of any air bubbles in the NOA resin, a bottom layer with a complementary negative-pattern and partial adhesive ability can be created through partial curing under UV irradiation for 2.5 mW/cm^2, 1 min (Vilber Lourmat VL-4.LC, 365 nm). The top block of the NOA device is prepared by molding it against the PDMS slab, where metal rods are inserted to retain the inlet and outlet for the NOA microfluidic device. Finally, each component of the NOA device is aligned and then mutually bonded through full curing under UV light for 2 hours.

3. Observation and Characterization

A cross-section of the positive-patterned PDMS replica is gained by vertically cutting the PDMS mold. Bright-field images are taken by a camera (Canon, EDS 6D, Japan) mounted on an optical microscope (Axiovert 200, Zeiss). The images are analyzed via computer software (Image J).

RESULTS AND DISCUSSION

1. Fabrication of the NOA Microfluidic Device

In this study, the fabrication protocol for NOA microfluidic devices is composed of two main steps. 1) Methyl group of PDMS surface is oxidized to be a silanol group by atmospheric-pressure plasma. The silanes can easily react with silanol group of substrate so that covalent bonds can be formed via vapor deposition [45]. A positive-patterned PDMS mold is generated from a silane-treated negative-patterned PDMS mold via replica molding (Fig. 1(a) and 1(b)). 2) The top and bottom sections of the NOA device are created using the positive-patterned PDMS mold and a PDMS slab with metal inserted via replica molding, and then bonded with each other (Fig. 1(c)). Following this method, NOA microfluidic devices are constructed using a positive-patterned silicon wafer, which is commonly used to fabricate PDMS microfluidic devices. This method minimizes the damage to the photoresist pattern on the silicon wafer because it can be accomplished without direct replica molding between the NOA and the silicon wafer. As most of the steps utilize replica molding, cheap NOA devices can be fabricated with a high throughput using the suggested protocol.

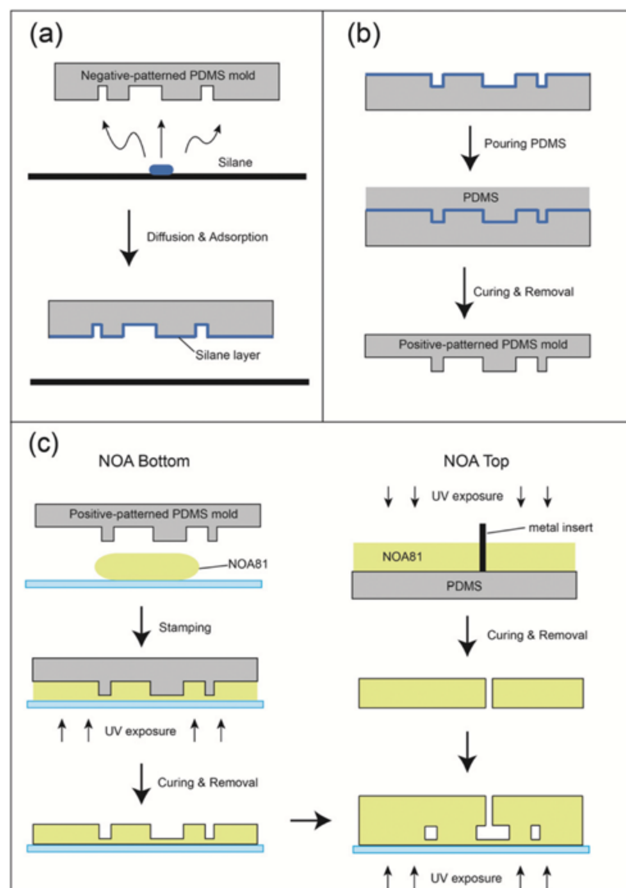

Fig. 1. Schematic diagram of the fabrication method for NOA microfluidic devices based on sequential replica molding.

2. Characterization of the Reproducibility of the PDMS Mold

Replica molding between PDMS and PDMS is required in this method. We experimentally analyzed the degree of cross-section deformation in PDMS patterns (Fig. 2). Fig. 2(a) depicts the cross-section of a negative-patterned PDMS mold and Fig. 2(b) presents the cross-section of a positive-patterned PDMS replica generated through replica molding using the PDMS template in Fig. 2(a). It is noted that width 1 slightly decreases by 9.56% (Fig. 2(c)) compared with the original width 1 of the PDMS mold. This results from the swelling of the mold due to the permeation of the liquid mixture with the 9 : 1 ratio of PDMS and curing agent. In the mixture, there are small molecules such as short PDMS polymeric chains and curing agents. These molecules can penetrate into the network of the PDMS template, causing the swelling of the template [46,47]. This mechanism occurs during the curing process of PDMS at 70 °C where the elevated temperature increases not only the permeability of the PDMS mold but also the diffusivity of the molecules [48]. Unfortunately, the swelling of the template does not occur isotropically but anisotropically. It is known that the degree of the swelling is different at the edge and surface [49]. The edge swells more than the surface because the edge has more contacting faces that can penetrate molecules through. The edge has two contact faces while the surface has one contacting face. The anisotropic shape of the PDMS replica shown in Fig. 2(b) is well explained by the anisotropic swelling. The length of the width 1 is determined by the length between the edges of negative-patterned PDMS mold. As the edges swell more than surfaces, the width 1 of the PDMS replica can be reduced more than the width 2. Despite the swelling of the mold, the width 2 and the height are very similar to those of the mold (Fig. 2(d) and 2(e)). The results show that the PDMS-PDMS replica molding process does not cause significant dimension difference between the original and replica PDMS molds.

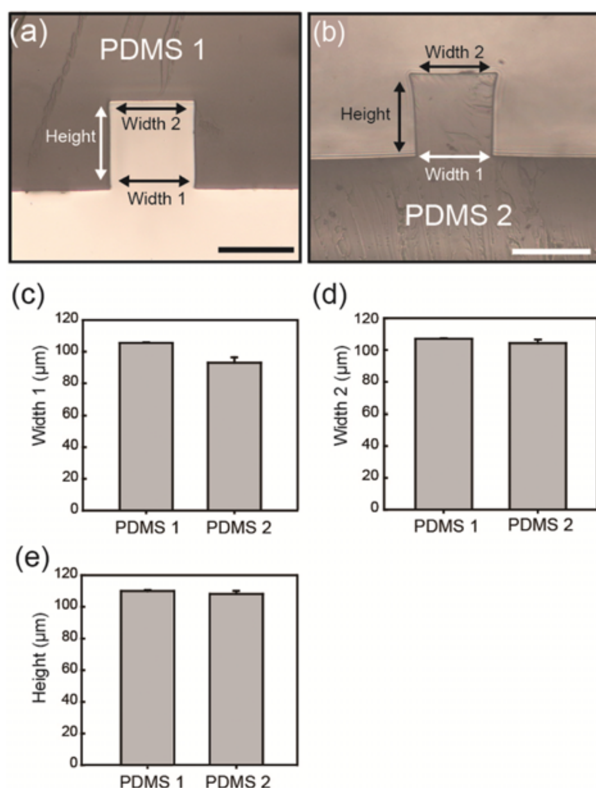

Fig. 2. The cross-sections of a negative-patterned PDMS template and a complementary positive-patterned PDMS replica. Bright-field images of the cross-section of (a) the negative-patterned PDMS mold and (b) the positive-patterned PDMS replica. A comparison of (c) width 1, (d) width 2, and (e) height of each PDMS mold (scale bars: 100 μm).

3. Characterization of the Repeatability of NOA Microfluidic Devices

Photoresist patterns on silicon wafers are easily damaged by the repetitive demolding of PDMS. This leads to an increase in cost and time as new silicon wafers need to be fabricated. To overcome this,

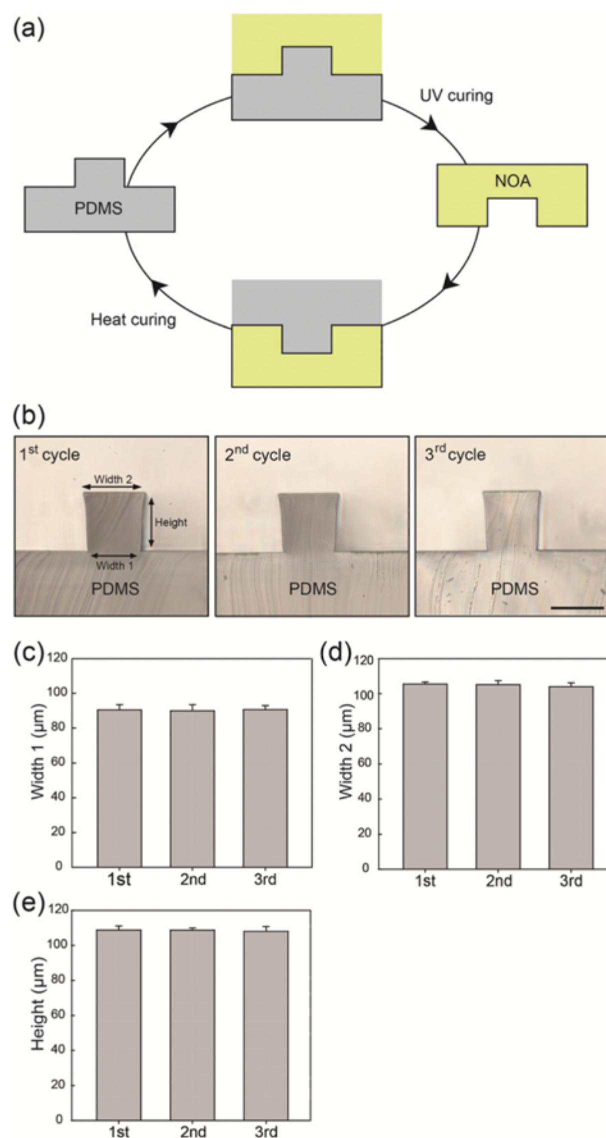

Fig. 3. (a) Schematic diagram of the cycle that enables the mass production of NOA microfluidic devices without replica molding using the wafer. (b) Bright-field images of the cross-sections of positive-patterned PDMS molds fabricated sequentially (scale bar: 100 μm). Analysis of (c) width 1, (d) width 2, and (e) height of each PDMS mold.

we develop a strategy that enables the mass production of NOA microfluidic devices using one negative-patterned PDMS replica. The negative-patterned PDMS mold acts as the master mold, eventually producing multiple negative-patterned NOA replicas.

This process involves producing a negative-patterned NOA replica from a positive-patterned PDMS replica, which can then itself be used to reproduce a positive-patterned PDMS replica. In this way, NOA microfluidic devices can be produced continuously (Fig. 3(a)). Fig. 3(b) presents a cross-section of a positive-patterned PDMS mold that is generated in this cycle. As shown in Fig. 3(c), there is no deformation of the pattern even after repeated production of NOA microfluidic devices.

4. NOA Microfluidic Devices with Various Geometries

The various micro-flow patterns are required to accomplish a number of experimental designs in microfluidic system. The flow patterns significantly depend on the geometries of microfluidic devices. In these reasons, it is important to simply give the diverse geometries to microfluidic devices based on the practical fabrication method. Here, through sequential replica molding, NOA microfluidic devices with various geometries can be easily constructed. NOA microfluidic devices can also be simply connected with several inlet or outlet types such as pipette tips, tygon tubes, and silicon tubes. Fig. 4 shows the several micro-flows developed in the NOA devices with various geometries. The red fluid is a solution of Rhodamine B and DI water, the blue fluid is a solution of food coloring and DI water, and the transparent flow is DI water. Fig. 4(a) presents three parallel multi-phase flows developed in a NOA device with three tube inlets and one tube outlet. Fig. 4(b) displays an extensional flow developed in a NOA device with one tube inlet and two tube outlets. Fig. 4(c) shows two vertically layered multiphase flows in a three-dimensional (3D) NOA device with pipette tip inlets and an outlet.

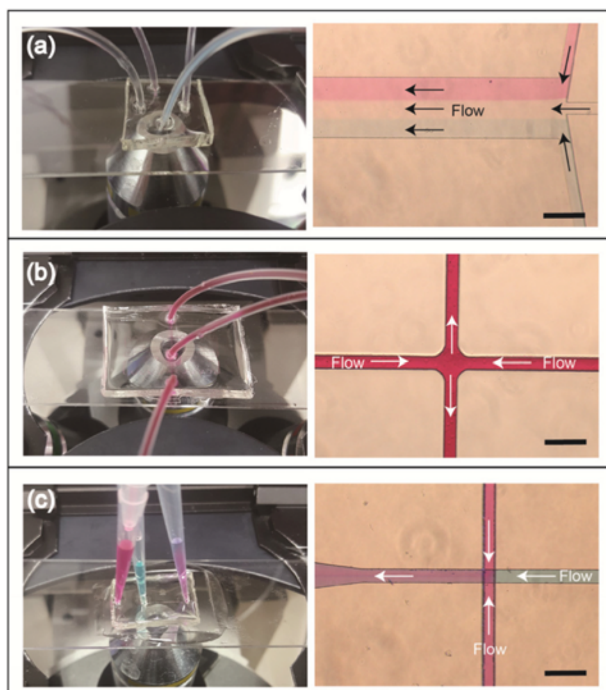

Fig. 4. (a) Bright-field image of parallel flows in a NOA microfluidic device. (b) Bright-field image of an extensional flow in a NOA microfluidic device. (c) Bright-field image of layered flows in a NOA microfluidic device (scale bar: 200 μm).

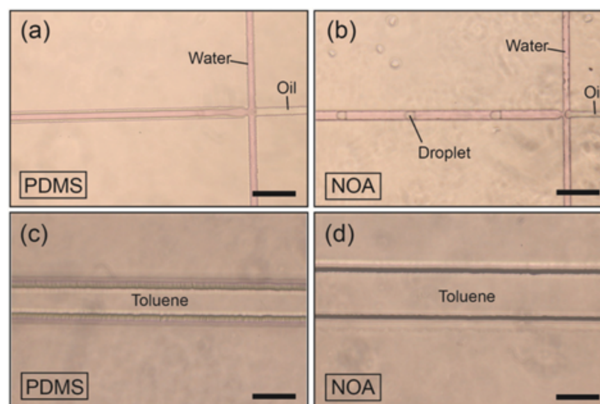

Fig. 5. Bright-field images of the oil-in-water droplet process in (a) a PDMS microfluidic device and (b) an NOA microfluidic device (scale bar: 200 μm). An aqueous red solution of Rhodamine B and a mineral oil are used for the continuous and disperse phases, respectively. Bright-field images of the geometry in the presence of toluene in (c) a PDMS microfluidic device and (d) an NOA microfluidic device (scale bar: 100 μm).

5. The Functionality of NOA Microfluidic Devices

We confirm that the NOA microfluidic devices produced from sequential replica molding are able to perform the same functions as other NOA devices outlined in previous studies. Of the many NOA device functions, we select two: an oil-in-water drop emitter, an organic solvent resist device. The stabilization of an emulsion in a microfluidic system, which has a high surface area to volume ratio, is affected by the wetting characteristics of the wall of the microfluidic device [50]. In the case of PDMS, a drop emitter cannot produce an oil-in-water emulsion because of its hydrophobic surface (Fig. 5(a)). To overcome this major limitation, oxygen plasma treatment of the PDMS can be applied. However, the PDMS surface usually regains its hydrophobicity after a few hours [23,24]. Contrary to PDMS drop emitters, NOA drop emitters can be used to successfully generate a monodisperse oil-in-water emulsion based on its hydrophilic surface (Fig. 5(b)). Figs. 5(c) and 5(d) present the geometric state around 30 min after the introduction of toluene to the PDMS and NOA microfluidic devices, respectively. The PDMS device swells in the presence of toluene (Fig. 5(c)), while the NOA device does not exhibit deformation because of its strong solvent resistance (Fig. 5(d)). This indicates that the strong organic solvent resistance of NOA devices can be achieved using our NOA microfluidic devices.

CONCLUSION

In this study, we propose a practical method for the fabrication of NOA microfluidic devices via sequential replica molding. Without the need for expensive equipment or complicated techniques, we are able to produce various 2D and 3D NOA microfluidic devices using a positive-patterned silicon wafer, which is generally used to

fabricate PDMS devices. We also analyze the deformation degree of the patterns during PDMS-PDMS replica molding and show that no significant deformation occurs. Moreover, we propose a strategy for the mass production of NOA devices using a single negative-patterned PDMS mold. The NOA devices fabricated by the sequential replica molding can be used in applications that are typically not possible with PDMS devices. We believe that our method can be a simple but powerful way to prepare NOA devices for a broad range of applications in various microfluidic systems.

ACKNOWLEDGEMENTS

This work was supported by the Engineering Research Center of Excellence Program through the National Research Foundation of Korea (NRF) funded by the Ministry of Science, ICT & Future Planning (NRF-2016R1A5A1010148), the Basic Science Research Program through the National Research Foundation of Korea (NRF) funded by the Ministry of Science, ICT & Future Planning (NRF-2015R1C1A1A02037452), and a grant from the Korea University.

REFERENCES

1. J. C. McDonald and G. M. Whitesides, *Acc. Chem. Res.*, **35**, 491 (2002).
2. D. Psaltis, S. R. Quake and C. Yang, *Nature*, **442**, 381 (2006).
3. Y. Hu and J. D. Mackenzie, *J. Mater. Sci.*, **27**, 4415 (1992).
4. S. W. Nam, D. Van Noort, Y. Yang and S. Park, *Lab on a Chip*, **7**, 638 (2007).
5. N. Y. Lee, Y. S. Yang, Y. S. Kim and S. S. Park, *Bull. Korean. Chem. Soc.*, **27**, 479 (2006).
6. A. J. Gawron, R. S. Martin and S. M. Lunte, *Electrophoresis*, **22**, 242 (2001).
7. D. Lee and K. H. Ahn, *Korea-Aust. Rheol. J.*, **27**, 65 (2015).
8. J. S. Hong, *Korea-Aust. Rheol. J.*, **28**, 77 (2016).
9. M. Dziubinski, *Korea-Aust. Rheol. J.*, **27**, 11 (2015).
10. J. W. Choi, K. W. Oh, J. H. Thomas, W. R. Heineman, H. B. Halsall, J. H. Nevin and C. H. Ahn, *Lab on a Chip*, **2**, 27 (2002).
11. J. Rossier, F. Reymond and P. E. Michel, *Electrophoresis*, **23**, 858 (2002).
12. L. Malic, D. Brassard, T. Veres and M. Tabrizian, *Lab on a Chip*, **10**, 418 (2010).
13. C. J. Bettinger, E. J. Weinberg, K. M. Kulig, J. P. Vacanti, Y. Wang, J. T. Borenstein and R. Langer, *Adv. Mater.*, **18**, 165 (2006).
14. N. W. Choi, M. Cabodi, B. Held, J. P. Gleghorn, L. J. Bonassar and A. D. Stroock, *Nat. Mater.*, **6**, 908 (2007).
15. H. Andersson and A. Van Den Berg, *Lab on a Chip*, **4**, 98 (2004).
16. P. Yager, T. Edwards, E. Fu, K. Helton, K. Nelson, M. R. Tam and B. H. Weigl, *Nature*, **442**, 412 (2006).
17. M. Seo, I. Gorelikov, R. Williams and N. Matsuura, *Langmuir*, **26**, 13855 (2010).
18. H. U. Kim, D. G. Choi, Y. H. Roh, M. S. Shim and K. W. Bong, *Small*, **12**, 3463 (2016).
19. Y. H. Roh, S. J. Sim, I. J. Cho, J. Choi, N. Choi and K. W. Bong, *Analyst*, **141**, 4578 (2016).
20. F. J. Blanco, M. Agirregabiria, J. Berganzo, K. Mayora, J. Elizalde, A. Calle and L. M. Lechuga, *J. Micromech. Microeng.*, **16**, 1006 (2006).
21. K. S. Hong, J. Wang, A. Sharonov, D. Chandra, J. Aizenberg and S. Yang, *J. Micromech. Micoreng.*, **16**, 1660 (2006).
22. J. N. Lee, C. Park and G. M. Whitesides, *Anal. Chem.*, **75**, 6544 (2003).
23. M. Morra, E. Occhiello, R. Marola, F. Garbassi, P. Humphrey and D. Johnson, *J. Colloid Interface Sci.*, **137**, 11 (1990).
24. J. L. Fritz and M. J. Owen, *J. Adhes.*, **54**, 33 (1995).
25. T. Gervais, J. El-Ali, A. Günther and K. F. Jensen, *Lab on a Chip*, **6**, 500 (2006).
26. B. S. Hardy, K. Uechi, J. Zhen and H. P. Kavehpour, *Lab on a Chip*, **9**, 935 (2009).
27. E. Delamarche, H. Schmid, B. Michel and H. Biebuyck, *Adv. Mater.*, **9**, 741 (1997).
28. C. F. Carlborg, T. Haraldsson, K. Öberg, M. Malkoch and W. van der Wijngaart, *Lab on a Chip*, **11**, 3136 (2011).
29. L. H. Hung, R. Lin and A. P. Lee, *Lab on a Chip*, **8**, 983 (2008).
30. D. Ogończyk, J. Węgrzyn, P. Jankowski, B. Dąbrowski and P. Garstecki, *Lab on a Chip*, **10**, 1324 (2010).
31. J. Chen, M. Wabuyele, H. Chen, D. Patterson, M. Hupert, H. Shadpour and S. A. Soper, *Anal. Chem.*, **77**, 658 (2005).
32. K. Ren, W. Dai, J. Zhou, J. Su and H. Wu, *Proc. Natl. Acad. Sci.*, **108**, 8162 (2011).
33. P. Kim, H. E. Jeong, A. Khademhosseini and K. Y. Suh, *Lab on a Chip*, **6**, 1432 (2006).
34. R. Barrett, M. Faucon, J. Lopez, G. Cristobal, F. Destremaut, A. Dodge and J. B. Salmon, *Lab on a Chip*, **6**, 494 (2006).
35. K. I. Min, T. H. Lee, C. P. Park, Z. Y. Wu, H. H. Girault, I. Ryu and D. P. Kim, *Angew. Chem. Int. Ed.*, **49**, 7063 (2010).
36. M. C. Park, J. Y. Hur, K. W. Kwon, S. H. Park and K. Y. Suh, *Lab on a Chip*, **6**, 988 (2006).
37. H. E. Jeong and K. Y. Suh, *Lab on a Chip*, **8**, 1787 (2008).
38. Z. T. Cygan, J. T. Cabral, K. L. Beers and E. J. Amis, *Langmuir*, **21**, 3629 (2005).
39. P. Wägli, A. Homsy and N. F. de Rooij, *Sens. Actuators, B*, **156**, 994 (2011).
40. E. Sollier, C. Murray, P. Maoddi and D. Di Carlo, *Lab on a Chip*, **11**, 3752 (2011).
41. K. W. Bong, J. Xu, J. H. Kim, S. C. Chapin, M. S. Strano, K. K. Gleason and P. S. Doyle, *Nat. Commun.*, **3**, 805 (2012).
42. D. Bartolo, G. Degré, P. Nghe and V. Studer, *Lab on a Chip*, **8**, 274 (2008).
43. K. Khanafer, A. Duprey, M. Schlicht and R. Berguer, *Biomed. Microdevices*, **11**, 503 (2009).
44. E. J. Lim, T. J. Ober, J. F. Edd, S. P. Desai, D. Neal, K. W. Bong and P. S. Doyle, *Nat. Commun.*, **5**, 4120 (2014).
45. B. Bhushan, D. Hansford and K. K. Lee, *J. Vac. Sci. Technol., A*, **24**, 1197 (2006).
46. J. E. Mark and Y. P. Ning, *Polym. Eng. Sci.*, **25**, 824 (1985).
47. Toepke, Michael W. and David J. Beebe., *Lab on a Chip*, **6**, 1484 (2006).
48. H. Zhang and A. Cloud, In Proceedings of 2006 SAMPE Fall Technical Conference (2006).
49. J. Pan, H. Chen, D. Zhang, X. Zhang, L. Yuan and L. Aobo, *J. Micromech. Microeng.*, **23**, 9 (2013).
50. R. Dreyfus, P. Tabeling and H. Willaime, *Phys. Rev. Lett.*, **90**, 144505 (2003).